Biochemical and Biophysical Research Communications 447 (2014) 231–236

Contents lists available at ScienceDirect

Biochemical and Biophysical Research Communications

journal homepage: www.elsevier.com/locate/ybbrc

Early senescence in heterozygous ABCA1 mutation skin fibroblasts: A gene dosage effect beyond HDL deficiency?

Mariarita Puntoni [a], Federico Bigazzi [b], Laura Sabatino [a], Francesco Sbrana [b], Antonio Musio [c], Beatrice Dal Pino [b], Andrea Ragusa [b], Elena Corsano [d], Tiziana Sampietro [b,*]

[a] CNR Institute of Clinical Physiology, Via Moruzzi n. 1, Pisa, Italy
[b] Fondazione Toscana Gabriele Monasterio, Via Moruzzi n. 1, Pisa, Italy
[c] Istituto di Ricerca Genetica e Biomedica, Consiglio Nazionale delle Ricerche, Via Moruzzi n. 1, Pisa, Italy
[d] Department of Clinical and Experimental Medicine, University of Pisa, Via Savi n. 6, Pisa, Italy

ARTICLE INFO

Article history:
Received 11 March 2014
Available online 26 March 2014

Keywords:
Tangier disease
β-Galactosidase
Telomere length
ATP-binding cassette transporter A1
ATP-binding cassette transporter G1
Low density lipoprotein receptor

ABSTRACT

Purpose: Homozygous ABCA1 gene mutation causes Tangier disease (TD). The effects reported in heterozygous state regard plasma HDL, cell cholesterol efflux and coronary artery disease. We investigated whether *in vitro* replicative skin fibroblast senescence shown in TD proband (Hom), his father (Het), and in a healthy control might be induced in a "gene-dosage way".
Methods: Senescence was evaluated by staining test for β-Galactosidase and telomere length (TL) on fibroblast DNA at different replicative stages. ABCG1 and LDLR (low density lipoprotein receptor) gene expression was also evaluated.
Results: Hom cells showed early senescent morphology and reduced growth at all passages *in vitro*. The cell positive percentage for β-Galactosidase test was highly increased in Hom compared to Het cells at late replicative status (66.1% *vs* 41.3% respectively). TL was significantly shorter at high stage either in Hom ($p < 0.0001$) or in Het ($p < 0.005$). At early replication cycles ABCG1 gene expression was about 3-fold higher in Hom compared to Het cells (0.44 *vs* 0.14 arbitrary unit).
Conclusions: ABCA1 gene mutation may have "gene-dosage way" effect on *in vitro* fibroblast senescence. Furthermore, increased ABCG1 and LDLR gene expression could highlight a role of ABCA1 on cytoskeleton regulation associated to cell cholesterol metabolism.

1. Introduction

Tangier disease (TD, *OMIM* 205400) is the most severe genetic form of HDL deficit. Its clinical phenotype is inherited as an autosomal recessive trait. TD is characterized by severe plasma deficiency or absence of HDL, apolipoprotein A-1 (apoA-1, the major HDL apolipoprotein) and by accumulation of cholesteryl esters in many tissues throughout the body [1,2]. This disorder is caused by mutations in the "ATP-Binding Cassette transporter A1" (ABCA1) gene [3], which encodes the membrane transporter ABCA1 [4–6]. This transporter plays a key role in the first step of reverse cholesterol transport (RCT), through which the efflux of free cholesterol (FC) from peripheral cells is transferred to lipid-poor apoA-1 [7] and thereby plays a central role in regulating cellular cholesterol homeostasis and in forming HDL.

Patients affected by TD are either homozygotes or compound heterozygotes depending on whether they carry two identical or two different mutant alleles of ABCA1 gene. Carriers of a single ABCA1 mutation (simple heterozygotes) display an intermediate phenotype with low HDL and about a 50% reduction in the ABCA1-mediated cell cholesterol efflux and have a co-dominant transmission [8].

Early studies assessed a major incidence of CAD in homozygous of Tangier kindred compared to heterozygous individuals and controls [9,10], supporting the hypothesis of the inverse correlation of HDL and CAD with homozygous null carriers with 35–65 years of age.

Subsequently, in large family studies, heterozygosis for mutations in ABCA1 was associated with increased carotid intimal thickening and displayed a greater than 3-fold increase in the CAD frequency than unaffected family members [11]. The altered cho-

Abbreviations: ABCA1, ATP-Binding Cassette transporter A1; FC, free cholesterol; Het, heterozygosis; Hom, homozygous; LDLR, low density lipoprotein receptor; RCT, reverse cholesterol transport; SA-β-gal, senescence-associated β-galactosidase; TD, Tangier disease; TL, telomere length.

* Corresponding author. Fax: +39 050 315 3030.
E-mail address: tiziana.sampietro@ftgm.it (T. Sampietro).

http://dx.doi.org/10.1016/j.bbrc.2014.03.090
0006-291X/

lesterol efflux is a plausible cell alteration to explain the strong proneness to CAD in TD patients, even though the association between the two conditions is not always satisfied.

Fibroblasts from TD patients have been shown to express the phenotype associated with accelerated senescence features such as enlarged morphology with altered actin-cytoskeletons [12,13], slow cell proliferation and increased staining for senescence-associated β-Galactosidase (SA-β-Gal) [14].

Data have accumulated to show that cellular senescence *in vitro* may be related to many human disorders including cardiovascular diseases [15].

A widely accepted mechanism of replicative senescence in human somatic cells, which is associated to aging *in vitro* is the telomere shortening [16,17]. Recent data pointed out the role of telomere length (TL) in mirroring the lifelong accumulation of oxidative stress and inflammation events [18], however, it is not totally clear which mechanisms are involved in determining the telomere shortening in cardiovascular disease [19].

The TD condition of accelerated atherosclerosis, so as accelerated senescence, is very intriguing and candidates this pathology as a natural model to elucidate the relation between senescence and atherosclerosis. It is possible to hypothesize that the mechanisms active in TD disease are the same that activate/facilitate both atherogenesis and accelerated senescence. To our knowledge, there are no data on the phenotype associated with cellular senescence in fibroblasts carrying ABCA1 heterozygosis.

We studied senescence in fibroblasts from a TD patient, his heterozygous father and a healthy control, analyzing their proliferation ability, the proliferating rate, the expression of SA-β-Gal and fibroblast telomere attrition at early, intermediate and late replicative status. The expression of ABCG1 and LDL receptor, the main actors of intracellular cholesterol in this condition was also studied in relation to the senescence curve.

2. Materials and methods

2.1. Patients

The subjects enrolled in the present study are a homozygous 34 year old male and his heterozygous father (56 year old) carrying a novel mutation of ABCA1 gene affecting the acceptor splice site of intron 20 (c.2961 −2 A > C) [20]. The main ABCA1 mutation induced traits, lipid profile and CAD, were present in lower severity in the two heterozygous family members: the proband's father and his 6 years old daughter had plasma HDL cholesterol, apoA-1 and apoA-2 half the normal levels. The father developed CAD later then proband and in less severe mode [1,2].

It is universally accepted to define TD syndrome only the homozygous state, however, for simplicity, we define homozygous and heterozygous TD forms.

2.2. Cell culture

Skin fibroblast lines were obtained from the Hom subject and his Het father. A cell line previously established in our laboratories served as control. All patients gave their informed consent.

The cells were cultured according to the standard conditions in modified Dulbecco Eagle's medium (DMEM) supplemented with l-glutamine, nonessential amino acids and 10% of fetal bovine serum in a humidified 5% CO_2 controlled incubator at 37 °C.

2.3. Cell proliferating rate

Replicative senescence, the phenomenon by which human cultured skin fibroblasts cease their proliferation and exhibit senescence after serial passaging, was analyzed by the modified method as described by Mathon et al. [15]. Fibroblasts (3×10^5 - cells) were plated onto 25 cm^2-plastic flacks (Corning Incorporated, NY, USA) under conditions described above. Every 2 days, cells were trypsinized and reseeded at a constant density. The cells were splitted to increase cumulative cell population doubling level (PDL). Three culture replicative stages were evaluated: early (PDL 6–11), intermediate (PDL 11–20) and late (PDL from 20th PDL).

2.4. Staining for senescence-associated β-Galactosidase

Cells were washed in PBS, fixed for 3–5 min (at room temperature) in 2% of paraformaldehyde, washed and incubated at 37 °C (without CO_2) with fresh senescence associated β-Gal (SA-β-Gal) stain solution: 1 mg of 5-bromo-4-chloro-3-indolyl P3-D-galactoside (X-Gal) per milliliter (stock = 20 mg of dimethylformamide/ml)/40 mM citric acid/sodium phosphate, pH 6.0/5 mM potassium ferrocyanide/5 mM potassium ferricyanide/150 mM NaCl/2 mM $MgCl_2$. Staining was evident in 2–4 h and maximal in 12–16 h. To detect lysosomal β-Gal, the citric acid/sodium phosphate was pH 4.0. Senescent cells are calculated as percentage of positive cells to β-Gal on the total fixed cells.

2.5. DNA and RNA extraction, and cDNA synthesis

DNA was extracted from the pellets obtained from fibroblasts at the three replicative stages: early, intermediate and late. DNA extraction was carried out with standardized procedure [21] with some modifications.

Total RNA was isolated from Hom and Het fibroblasts by RNeasy Midi Kit (Qiagen, Valencia, CA, USA) following the supplied protocols. Tissue homogenization was performed using Tissue Lyser (Qiagen, Valencia, CA, USA). Purified RNA was quantified using NanoDrop (Celbio, Mi, Italy). RNA purity and integrity were evaluated by checking the absorbance ratios A260/280 and A260/230 and assessing the sharpness of 18S and 28S ribosomal RNA bands on 1% agarose gel stained with GelRed™ (Biotium, Hayward, CA). RNA samples were stored at −80 °C until use. Genomic DNA elimination and reverse transcription were performed using QuantiTect Reverse Transcription Kit (Qiagen, Valencia, CA, USA) following the supplied protocol. The obtained cDNA samples were stored at −20 °C until use.

2.6. Real time PCR

Real time amplification reactions (45 cycles) were performed using Rotor-Gene 3000 (Corbett) by adding 2 μl of 10-fold diluted cDNA and 400 nM of each primer to a real-time PCR supermix (SsoFast EvaGreen Supermix, Bio-Rad, Hercules, CA, USA). The utilized amplification program was the one suggested by the supplied manual.

Primer pairs specific for ABCG1, LDLR, β-actin are reported in table 1 along with the relative annealing temperatures. All the primer pairs were designed with the Beacon Designer 5.0 software and synthesized by MMedical (St. Louis, MO, USA). β-Actin was utilized as endogenous controls to normalize for RNA loading or differences in reverse transcription efficiency. Primer pairs were tested with different temperatures to find the best annealing temperature. Before performing real time PCR experiments, each primer pair was checked performing a standard RT-PCR reaction. The amplified DNA fragments were separated on 1% agarose gel stained with GelRed™ (Biotium, Hayward, CA) and visualized under ultraviolet light.

Table 1
Primers pairs and annealing temperature for real time RT-PCR experiments.

Gene	Forward (5′ → 3′)	Reverse (5′ → 3′)	Annealing *T* (°C)
β-Actina	CAACTCCATCATGAAGTGTGACG	TCAGGAGGAGCAATGATCTTGATC	60
ABCG1	AACGAAGCCAAGAAGGTC	CCAGTAGTTCAGGTGTTCC	55
LDLR	ACGGTGGAGATAGTGACAATG	AGACGAGGAGCACGATGG	58

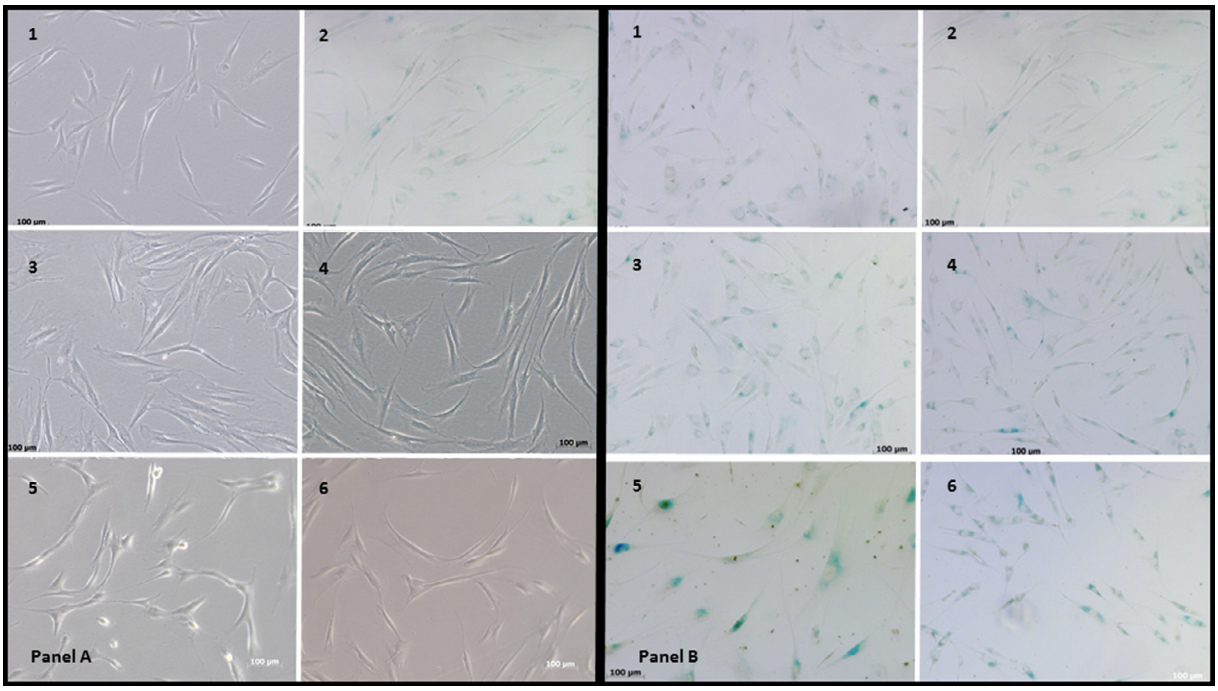

Fig. 1. Panel A. Representative pictures for Hom and Het fibroblasts at Optical Microscopy at early replicative status (PDL6), (panel 1 Hom, panel 2 Het); at intermediate replicative status (PDL11) panel 3 Hom, panel 4 Het; at late replicative status (PDL20), panel 5 Hom, panel 6 Het. Panel B. Representative pictures for SA-β-Gal positive fibroblasts. (1) Hom early replicative status (PDL8), (2) Het early replicative status (PDL9), (3) Hom intermediate replicative status (PDL17), (4) Het intermediate replicative status (PDL17), (5) Hom late replicative status (PDL22), (6) Het late replicative status (PDL21).

2.7. Detection of relative telomere length by monochrome multiplex quantitative PCR (MMQPCR) method

MMQPCR was performed according the method described previously [22,23]. MMQPCR was carried out into a 384-well CFX RT-PCR System (Bio-Rad) in a 10 μl reaction mix containing 10–20 ng of genomic DNA in 1x iQ SYBR Green Supermix (Bio-Rad). Each sample was assayed in triplicates in three different runs, with negative and positive controls included. A standard curve for telomere and β-globin (or single copy gene, SCG) combination was also evaluated in each assay as control of amplification efficiency and linearity.

3. Results

Hom fibroblasts failed to reach confluence despite regular refeeding at 30th passage, initiating to slow the proliferation rate as yet at passage 20–22 when they also showed the morphologic characteristics of senescent cells: enlarged and flattened shape. For the Het fibroblasts passage 30 is the first step of aging in that they start to slow replication and to show the morphologic alterations, while PDL 30 control fibroblasts still show a constant proliferation rate (Fig. 1A).

3.1. SA-β-Gal staining

Hom and Het fibroblasts where analyzed for the expression of the specific isoform of SA-β-Gal. Hom and Het fibroblasts were compared to the health's control (data not shown). In Fig. 1B representative pictures of SA-β-Gal staining in Hom and Het fibroblasts are reported. In Fig. 2, SA-β-Gal is much more evident in Hom than in Het, and increased in parallel with PDL; at late PDL the Hom SA-β-Gal positive is 66.1% *vs* 41.3% of Het cells. SA-β-Gal in healthy control is not shown.

3.2. Detection of the relative TL by MMQPCR method

Real-Time PCR amplification efficiency and linearity: for the evaluation of the effective efficiency, a standard curve was performed and efficiencies and curves slopes were calculated by the CFX software automatically. Four concentrations with 3-fold serial dilutions of human genomic DNA obtained from a mix of analyzed samples were prepared (40 ng, 13.3 ng, 4.4 ng, 1.5 ng per well) in triplicates in each plate. The average PCR efficiency was 2.8 for the telomere and 2.0 for the SCG. The two independent standard curves, one for telomere sequences and another for SCG were obtained by acquiring SYBR Green fluorescence signal at two different temperatures, 74 °C for telomere and 88 °C for SCG, in each cycle of stage 3 of the cycling protocol. The relative telomere length (T/S ratio) for each sample was calculated using the ΔΔCt method with the Pfaffl correction and the relative ΔCt for each sample was determined using the mean of Ct for all wells in the plate as control, as previously described [23,24].

The relative quantification with the MMQPCR showed that the TL (expressed as T/S ratio) was significantly shorter at high replicative stage (PDL 23 for Hom and PDL 21 for Het) when compared to early replicative stage (PDL 6 for Hom and PDL 5 for Het) either in

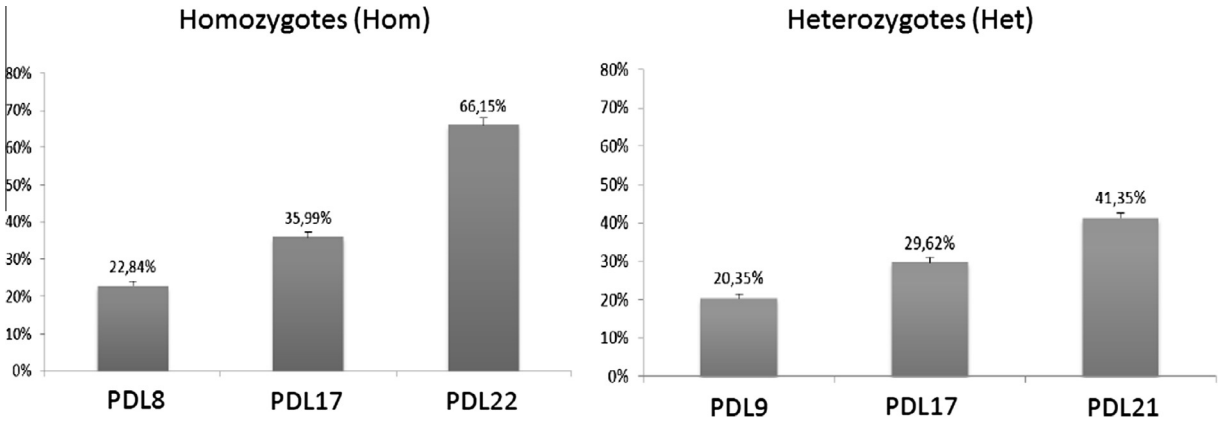

Fig. 2. SA- β-Gal staining in Hom and Het fibroblasts. Senescent cells of Hom (A) and Het (B) are calculated as percentage of positive cells to as percentage of positive cells β-Gal respect to total fixed cells. Senescent cells are calculated at three different replicative status.

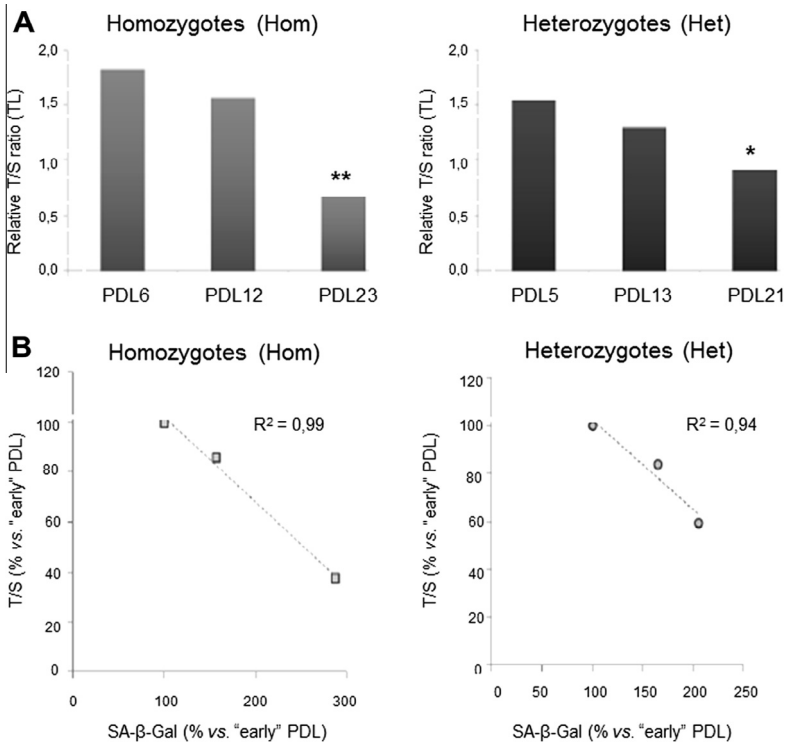

Fig. 3. Panel A. Relative quantifications of TL (with MMQPCR) in Hom and Het fibroblasts. TL (expressed as T/S ratio) is calculated at three different replicative status.*$p < 0.05$; **$p < 0.0001$, data are referred to early replicative status values PDL6 (Hom) and PDL5 (Het). Panel B. Correlation plot representing increased SA-β-Gal staining *vs* decreased telomere length in Hom and in Het. All values are expressed as percentage respect to the early replicative status. Hom: $R^2 = 0.99$; Het: $R^2 = 0.94$.

Hom ($p < 0.0001$) or in Het ($p < 0.05$), while no significant decrease was detected at intermediate replicative stage (Fig. 3A). Moreover, a very strong correlation ($R = 0.99$) was found between increased SA-β-Gal staining and decreased telomere length throughout PDL stages (all data were expressed as percentage respect to the early replicative status). A correlation plot is represented in Fig. 3B.

3.3. ABCG1. and LDLR expression

As illustrated in Fig. 4A, ABCG1 gene expression in Hom fibroblasts was higher respect to Het cells; at early replication cycles in Hom it was 3-fold (0.44 *vs* 0.14 arbitrary unit). This difference decreased along with the PDL increase.

Concerning the LDLR gene expression, there was no difference between the Hom and Het cells while a trend in an increased expression in parallel with the increase PDL can be appreciated (Fig. 4B).

4. Discussion

In the present study, we showed that fibroblast are early senescent also in heterozygous state. Furthermore we confirmed data previously reported on the Hom fibroblasts [14].

Het fibroblasts senescence is earlier than control and later than Hom, and suggested a progression in the severity of disease related to HDL deficiency, as outlined for CAD and HDL plasma concentration [11,25].

Telomere shortening is one of the main marker of cellular senescence, and telomere attrition has been widely demonstrated to be emphasized during the aging process [16]. In the present

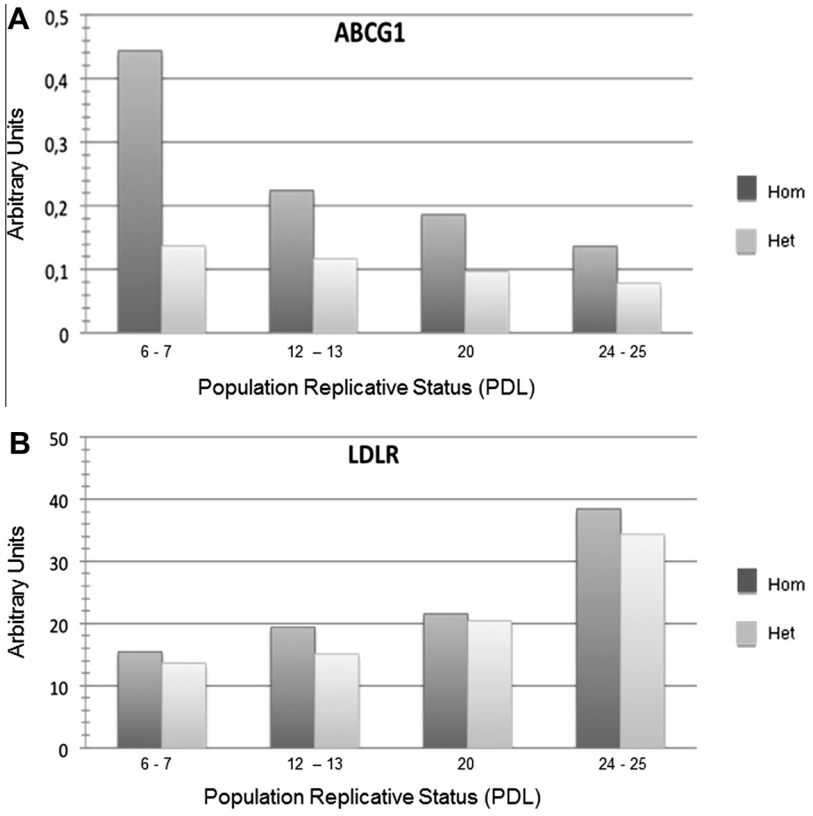

Fig. 4. Panel A. ABCG1 gene expression in Hom and Het fibroblasts. ABCG1 expression is in arbitrary units. PDL (population doubling level) has been analyzed at early (6–7) intermediate (12–13 and 20) and late (24–25) replicative status. Panel B. LDLr gene expression in Hom and Het fibroblasts. Hom Het fibroblasts; gene expression expressed in arbitrary units PDL population replicative status.

study, we found that telomere shortening is strongly associated to the fibroblast PDL, resulting significantly shorter at late passages. This finding is in agreement with previous data on telomere shortening in TD homozygous patients [14]. Interestingly, we found that progression of telomere resulted 1.5-fold more pronounced in Hom than in Het patient (Fig. 3A).

The accelerated senescence demonstrated on fibroblasts could have an explanation by the altered actin-cytoskeleton [26] regulation, which, among the others, is a function under the ABCA1 gene control [27].

We considered that the absence of activity of ABCA1 gene could have a reflection on the two other main genes regulating the cell cholesterol content, ABCG1 and LDLR genes. We found that the ABCG1 expression in Hom was higher than in Het suggesting the existence of a compensatory mechanism of the cells aiming to promote the cholesterol efflux. Furthermore, this hypothesis is supported by the increased expression of ABCG1 in TD patients macrophages. The LDLR expression was not different in Hom vs Het, but it tended to increase with the cell aging.

The increasing trend for LDLR mRNA in Hom and Het fibroblasts from early to late replicative status, was probably due to a dis-regulation associated to the cell senescence events. Therefore, the excess of esterified cholesterol in the ABCA1 mutated cells, could cause a decrease, rather than an increase, in the genes expression related to the cholesterol intake.

In summary, our data pointed out that the skin fibroblasts obtained from patients with heterozygosis for mutations in ABCA1 showed a senescent phenotype in the intermediate replicative status respect to TD and control. Furthermore, the parallel ABCG1 and LDLR gene expression increase could highlight a possible role of ABCA1 gene on cytoskeleton regulation related to cell cholesterol metabolism.

Future studies will be needed to better understand the cellular dynamics that link chronic inflammatory events to cellular senescence in premature CAD in order to step forward in the development of new approaches for prevention and treatment.

References

[1] T. Sampietro, M. Puntoni, F. Bigazzi, et al., Tangier disease in severely progressive coronary and peripheral artery disease, Circulation 119 (2009) 2741–2742.
[2] M. Puntoni, F. Sbrana, F. Bigazzi, et al., Tangier disease: epidemiology, pathophysiology and management, Am. J. Cardiovasc. Drugs 12 (2012) 303–311.
[3] L.R. Brunham, R.R. Singaraja, M.R. Hayden, Variation on a gene: rare and common variants in ABCA1 and their impact on HDL cholesterol levels and atherosclerosis, Annu. Rev. Nutr. 26 (2006) 105–129.
[4] A. Brooks-Wilson, M. Marcil, S.M. Clee, et al., Mutations in ABC1 in tangier disease and familial high-density lipoprotein deficiency, Nat. Genet. 22 (1999) 336–345.
[5] M. Bodzioch, E. Orso, J. Klucken, et al., The gene encoding ATP-binding cassette transporter 1 is mutated in tangier disease, Nat. Genet. 22 (1999) 347–351.
[6] S. Rust, M. Walter, H. Funke, et al., Tangier disease is caused by mutations in the gene encoding ATP-binding cassette transporter 1, Nat. Genet. 22 (1999) 352–355.
[7] J.F. Oram, A.M. Vaugham, ATP-binding cassette cholesterol transporters and cardiovascular disease, Circ. Res. 99 (2006) 1031–1043.
[8] M.E. Brousseau, E.J. Schaefer, J. Dupuis, et al., Novel mutations in the gene encoding ATP binding cassette 1 in four tangier disease kindreds, J. Lipid Res. 41 (2000) 433–441.
[9] H.N. Hoffman, D.S. Fredrickson, Tangier disease (familial high density lipoprotein deficiency). clinical and genetic features in two adults, Am. J. Med. 39 (1965) 582–593.
[10] E.J. Schaefer, L.A. Zech, D.E. Schwartz, et al., Coronary heart disease prevalence and other clinical features in familial high-density lipoprotein deficiency (Tangier disease), Ann. Intern. Med. 93 (1980) 261–266.
[11] S.M. Clee, J.J.P. Kastelein, M. van Dam, et al., Age and residual cholesterol efflux affect HDL cholesterol levels and coronary artery disease in ABCA1 heterozygotes, J. Clin. Invest. 106 (2000) 1263–1270.
[12] K. Hirano, F. Matsuura, K. Tsukamoto, et al., Decreased expression of a member of the Rho GTPase family, Cdc42Hs, in cells from Tangier disease – the small G protein may play a role in cholesterol efflux, FEBS Lett. 484 (2000) 275–279.

[13] W. Drobnik, G. Liebisch, C. Biederer, et al., Growth and cell cycle abnormalities of fibroblasts from Tangier disease patients, Arterioscler. Thromb. Vasc. Biol. 19 (1999) 28–38.
[14] F. Matsuura, K. Hirano, C. Ikegami, et al., Senescent phenotypes of skin fibroblasts from patients with tangier disease, Biochem. Biophys. Res. Commun. 357 (2007) 493–498.
[15] N.F. Mathon, D.S. Malcolm, M.C. Harrisingh, et al., Lack of replicative senescence in normal rodent glia, Science 291 (2001) 872–875.
[16] K.D. Salpea, C.G. Maubaret, A. Kathagen, et al., The effect of pro-inflammatory conditioning and/or high glucose on telomere shortening of aging fibroblasts, PLoS One 8 (2013) e73756.
[17] J. Campisi, S.H. Kim, C.S. Lim, et al., Cellular senescence, cancer and aging: the telomere connection, Exp. Gerontol. 36 (2001) 1619–1637.
[18] W. Chen, J.P. Gardner, M. Kimura, et al., Leukocyte telomere length is associated with HDL cholesterol levels: the bogalusa heart study, Atherosclerosis 205 (2009) 620–625.
[19] T. von Ziglinicki, Oxidative stress shortens telomeres, Trends Biochem. Sci. 27 (2002) 339–344.
[20] L. Bocchi, L. Pisciotta, T. Fasano, et al., Multiple abnormally spliced ABCA1 mRNAs caused by a novel splice site mutation of ABCA1 gene in a patient with Tangier disease, Clin. Chim. Acta 411 (2010) 524–530.
[21] J. Sambrook, E.F. Fritsch, T. Maniatis, Molecular Cloning: A Laboratory Manual, second ed., Cold Spring Harbor Laboratory Press, Cold Spring Harbor, Plainview, NY, New York, NY, USA, 1989.
[22] R.M. Cawthon, Telomere length measurements by a novel monochrome multiplex quantitative PCR method, Nucleic Acids Res. 37 (2009) e21.
[23] L. Sabatino, N. Botto, A. Borghini, et al., Development of a new multiplex quantitative real-time PCR assay for the detection of the mtDNA(4977) deletion in coronary artery disease patients: a link with telomere shortening, Environ. Mol. Mutagen. 4 (2013) 299–307.
[24] M.W. Pfaffl, A new mathematical model for relative quantification in real-time RT-PCR, Nucleic Acid Res. 29 (2001) e45.
[25] R. Frikke-Schmidt, Genetic variation in the ABCA1 gene, HDL cholesterol, and risk of ischemic heart disease in the general population, Atherosclerosis 208 (2010) 305–316.
[26] K. Tsukamoto, K. Hirano, K. Tsujii, et al., ATP-binding cassette transporter-1 induces rearrangement of actin cytoskeletons possibly through Cdc42/N-WASP, Biochem. Biophys. Res. Commun. 287 (2001) 757–765.
[27] R.J. Aiello, D. Brees, O.L. Francone, ABCA1-deficient mice: insights into the role of monocyte lipid efflux in HDL formation and inflammation, Arterioscler. Thromb. Vasc. Biol. 23 (2003) 972–980.